



3D Quantitative MRI: A Fast and Reliable Method for Ventricular Volumetry

Rafael T. Holmgren¹, Anders Tisell^{2,3}, Marcel J.B. Warntjes^{3,4}, Charalampos Georgiopoulos^{3,5}

■ **PURPOSE:** Volumetry of cerebral ventricles is a far more sensitive measure for shunt-induced reduction of ventricular size than traditional 2-dimensional (2D) measures, such as Evans index. However, available ventricle segmentation methods are time-consuming, resulting in limited use in clinical practice. Quantitative MRI (qMRI) obtains objective measurements of physical tissue properties, enabling automatic segmentation of white and gray matter and intracranial cerebrospinal fluid. The aim of this study was to evaluate the reliability and processing time of both manual and manually corrected automatic ventricular volumetry through the application of 3D qMRI.

■ **METHODS:** An independent examiner performed manual ventricular volumetry segmentations on 45 3D qMRI acquisitions (15 healthy individuals, 15 idiopathic normal pressure hydrocephalus (iNPH) patients, 15 shunted iNPH patients) twice. Another independent examiner manually segmented 15 of these acquisitions once. An automatic ventricle segmentation algorithm generated a third set of ventricular segmentations for all 45 data sets. The automatic segmentations were then corrected by both examiners to obtain a fourth set of data. All segmentations were assessed for intra- and interobserver reliability.

■ **RESULTS:** Intra- and interobserver reliability for all segmentations, manual, corrected, and automatic, was excellent (intra-class correlation coefficient 1.000, 1.000 and 0.999 respectively). Ventricular volumes were on average 42 ± 18 mL (mean \pm SD) in healthy individuals, 140 ± 34 mL in iNPH patients, and 113 ± 35 mL in shunted iNPH patients.

■ **CONCLUSIONS:** 3D qMRI is a reliable and time-efficient method to obtain relevant volumetric measures of intracranial cerebrospinal fluid spaces for both clinical and research purposes. The corrected automatic segmentations provide a feasible time expenditure for clinicians caring for patients with iNPH.

INTRODUCTION

Hydrocephalus is a disease with ventriculomegaly due to disturbed cerebrospinal fluid (CSF) dynamics. There are many causes, subgroups, and variation in terms of symptom severity and degree of ventriculomegaly. Various types of hydrocephalus differ in post-shunting brain compliance, with

Key words

- Evan's index
- Idiopathic normal pressure hydrocephalus
- Neuroimaging
- Quantitative MRI
- Ventricular volumetry
- Volumetry

Abbreviations

- 3D-QALAS:** 3D-quantification using an interleaved Look-Locker acquisition sequence with T2 preparation pulse
- BPF%:** Brain parenchymal fraction
- BPV:** Brain parenchyma volume
- CA:** Callosal angle
- CSF:** Cerebrospinal fluid
- CT:** Computed tomography
- EI:** Evans index
- ICC:** Intraclass correlation coefficient
- ICV:** Intracranial volume
- iNPH:** Idiopathic normal pressure hydrocephalus

MRI: Magnetic resonance imaging

qMRI: Quantitative MRI

ROI: Region of interest

From the ¹Departments of Neurosurgery, Biomedical and Clinical Sciences, Linköping University, Sweden; ²Departments of medical radiation physics, health and caring sciences, Linköping University, Sweden; ³Center for medical image science and visualization (CMIV), Linköping University, Sweden; ⁴SyntheticMR AB, Linköping, Sweden; and ⁵Diagnostic Radiology, Department of Clinical Sciences, Medical Faculty, Lund University, Sweden

To whom correspondence should be addressed: Rafael T. Holmgren, M.D.
[E-mail: rafael.holmgren@liu.se]

Citation: *World Neurosurg.* (2025) 195:123661.
<https://doi.org/10.1016/j.wneu.2025.123661>

Journal homepage: www.journals.elsevier.com/world-neurosurgery

Available online: www.sciencedirect.com

1878-8750/© 2025 The Author(s). Published by Elsevier Inc. This is an open access article under the CC BY license (<http://creativecommons.org/licenses/by/4.0/>).

substantial variation in the ability of ventricles to decrease in volume even after successful shunt surgery or endoscopic surgical intervention, when measured with traditional radiographic measures. Such inability is particularly pronounced in certain types of hydrocephalus, such as in idiopathic normal pressure hydrocephalus (iNPH).^{1,2}

Traditional radiologic methods often lack sensitivity to detect ventricular change, which is important in longitudinal follow-up. Two-dimensional (2D) metric measures, such as frontal horn width and Evans index (EI), have been in use since the era of pneumoencephalography and were later translated into the computed tomography (CT) and magnetic resonance imaging (MRI) era.^{3,4} EI greater than 0.3 is a prerequisite for the diagnosis of iNPH according to international guidelines.⁵ Unfortunately, EI has significant weaknesses, as hydrocephalus can be unequally distributed across the ventricular system (e.g., with patients having more widened occipital than frontal horns).⁶ Moreover, EI is often unchanged after successful shunt surgery in iNPH and also in cases of shunt failure.¹

Ventricular volumetry has long been a research tool in dementia and hydrocephalus studies and has recently been studied for aging-related volume changes and establishment of age- and sex-specific reference values.^{7,8} It is proven to be more sensitive for changes in ventricular volume compared with 2D metric measures.⁹ There are numerous segmentation software tools available for the volumetric post-processing of conventional 3D MRIs, most of which rely on isotropic T₁-weighted sequences.^{10–14} Many of these also include automated segmentations of brain structures including the ventricles. However, ventricular volumetry has not yet gained popularity in clinical practice due to methodologic obstacles, including often complex software and the time-consuming nature of manual segmentation.¹⁵

Quantitative MRI (qMRI), which enables simultaneous quantification of T₁ and T₂ relaxation times and proton density with high reliability,¹⁶ has been used in assessment of normal development, aging, and a variety of neurological diseases.¹⁷ qMRI protocols can generate any contrast-weighted image used in routine clinical settings, a process called synthetic MRI. An important advantage of qMRI lies in its ability to automatically determine the intracranial volume (ICV) and segment specific intracranial tissues such as white matter, gray matter, myelin, and CSF.^{18,19} 3D-quantification using an interleaved Look-Locker acquisition sequence with T₂ preparation pulse (3D-QALAS) is a novel qMRI sequence, which has been validated for the reproducibility and repeatability of brain volumetric measurements in both human and phantom models by Fujita et al.^{20,21} The acquisition time for 3D-QALAS is 6 minutes and the acquired images can be visualized in several different contrasts, such as myelin maps or CSF maps. Starting with CSF maps expedites the process of manual ventricle segmentation. Instead of meticulously outlining ventricular borders, the ventricles can be roughly outlined with a large region of interest (ROI). Subsequently, all CSF within this ROI is seamlessly integrated into a ventricular CSF map, streamlining the process. 3D-QALAS is commercially available on Philips, Siemens, GE, and Cannon equipment. The sequence is not yet regulatory approved for clinical use but can be obtained as a “work-in-progress” sequence.

With the aforementioned advantages of qMRI, 3D-QALAS holds the potential to serve as a rapid and reliable segmentation tool in

the field of ventricular volumetry. However, there is to date no clinical qMRI application for manual or automatic ventricle volume measurements. The aim of this study was to evaluate the reliability and efficiency of qMRI in assessing the volume of the ventricular system in its entirety, both manually and after the application of an automatic segmentation algorithm.

METHODS

Study Population

At our institution, 50 iNPH patients deemed suitable for shunt surgery underwent consecutive recruitment between January 2021 and July 2022. Fifty age-matched healthy controls were also recruited in this cohort, either through advertisements in local newspapers or via patients' spouses. The recruitment process and data collection were approved by the Swedish Ethical Review Authority (ref. no. 2020–00719) and all participants provided written informed consent upon enrollment. Patients underwent MRI examination the day before surgery and 3 months postoperatively. Healthy controls were examined once. For the purposes of this study, MRI scans were randomly selected using a computer-generated random number among the total number of 50 scans in each group. Specifically, 15 exams were selected from iNPH patients who were examined the day before surgery, 15 from iNPH patients examined 3 months after shunt surgery, and 15 from healthy controls. Our rationale for selecting patients both with and without shunt was to investigate whether ventricular segmentation with qMRI might be compromised by shunt artifacts. We opted for a random selection of patients across these 2 stages, since assessing the efficacy of the shunting procedure fell outside the scope of this study. In total, 45 MRI scans were used in this study. The sample size was determined based on earlier similar study cohorts.^{16,19,21,22} All shunted patients were operated with a Codman CERTAS Plus valve system (Integra LifeSciences, Princeton, New Jersey, USA).^{23–25} To ensure blinded MRI assessment, all patient data was anonymized. INPH patients were examined clinically according to the Hellstrom iNPH scale preoperatively and 3 months postoperatively, comprising domains of gait, balance, cognition, and urinary incontinence.²⁶

qMRI Acquisition

Individuals were examined on a 3T Siemens Prisma MR scanner (Erlangen, Germany) with a 20-channel head coil. Image acquisition included T₁-weighted images, T₂-weighted images, and an in-house developed prototype version of 3D-QALAS.²⁷ 3D-QALAS consists of 5 parallel, segmented 3D turbo field echo gradient echo acquisitions interleaved with T₂ preparation pulses and inversion pulses, measuring the T₁ and T₂ relaxation times and proton density.²⁸ Based on these maps the partial volume of CSF per voxel was automatically calculated using the image analysis software SyMRI v0.45.36 (SyntheticMR AB, Sweden).²⁹ A full-coverage, 1.20x1.23 × 1.23 mm isotropic resolution was obtained in a scan time of 6 minutes.

Manual Volumetric qMRI Segmentation Assessment

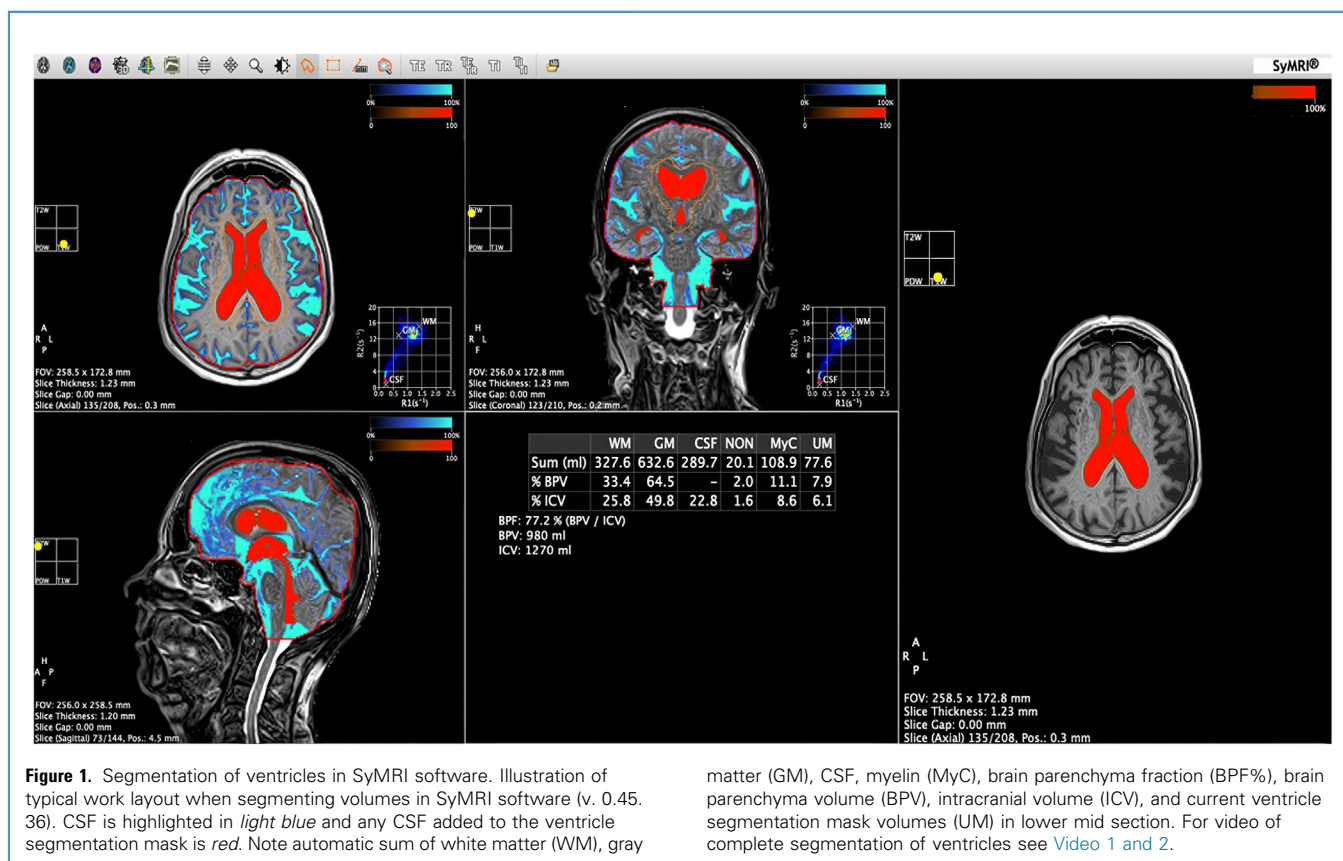
Volumetric measurements were conducted using 3D-QALAS data, on synthetic T₁- or T₂-weighted images generated using the SyMRI software. CSF was highlighted as color overlays on the

synthetic T1- and T2-weighted images and were expressed in partial volume in the range 0%–100% of each reconstructed voxel. Manual segmentation was performed on axial, coronal, and sagittal planes. Each examiner assessed ventricular CSF volumes from extraventricular spaces by manually tracing an ROI around the ventricles. Adding CSF within a drawn ROI removes the need to delineate the ventricular borders in detail. This saves time for manual segmentation and is regarded as a main advantage of quantitative MRI. A “magic wand” tool was also used to collect CSF within a confluent area clearly inside the brain ventricles. All CSF within the ROI or suggested by the “magic wand” was then added to the ventricle segmentation mask (reflecting ventricular CSF volume). The software automatically calculates and displays the following parameters: ICV, brain parenchyma fraction (BPF%), intracranial CSF volume, and brain parenchyma volume (BPV). We have additionally calculated the ratio between ventricle segmentation mask and total CSF on non-shunted and healthy volunteers. However, precise calculations of ICV, BPV, and BPF% and ventricular/total CSF ratio were not feasible in shunted INPH patients due to artifacts from the Codman Certas Plus shunt valve. **Figure 1** illustrates a segmentation example, showcasing the delineation process of ventricular volume and including the generated table with all calculated volumes. For a video of the manual segmentation process see Video 1.

All 45 scans underwent manual ventricle segmentation by a neurosurgeon twice (test and retest) to calculate intraobserver reliability (R.H. – assessor 1). A neuroradiologist (C.G. – assessor 2) independently assessed 15 scans (5 randomly selected from each group) to calculate interobserver reliability. Assessment time for all segmentations was recorded. Moreover, assessor 2 evaluated all scans using Radscale, a rating system that incorporates both EI and callosal angle (CA), using conventional MRI sequences.³⁰

Automatic Volumetric qMRI Segmentation Assessment

An automatic ventricle segmentation algorithm was developed using the first set of segmentations by assessor 1 as a template. Automatic segmentation of the ventricular system was performed based on the CSF maps using a patched version of SyMRI. The time for post-processing was less than 1 second. The lateral ventricles were seeded in the mid-coronal slice followed by region-growing along high partial volume CSF. Then the fourth ventricle was seeded on the posterior side of the brain stem followed by region growing. The region growing was allowed to pass through the aqueduct to the third ventricle. Finally, the third ventricle was added by further region growing, restricted by the lamina terminalis and the posterior commissure. Care was taken to connect the third and lateral ventricles via the foramen of Monro. The post-processing was mainly tissue-based and included only a



matter (GM), CSF, myelin (MyC), brain parenchyma fraction (BPF%), brain parenchyma volume (BPV), intracranial volume (ICV), and current ventricle segmentation mask volumes (UM) in lower mid section. For video of complete segmentation of ventricles see Video 1 and 2.

minimum of geometrical restrictions to avoid limited segmentation due to irregular shapes. The algorithm was applied to all 45 scans and a set of automatic volume assessments was generated. These were compared to the corresponding manual segmentations of both assessors for interobserver reliability.

Manually Corrected Volumetric Segmentation Assessment

To verify the accuracy of the automatic algorithm, both assessors manually corrected the automatic set of volumetric data, by adding missing parts of the ventricles and erasing non-ventricular voxels. The time taken for these corrections was recorded. These corrected segmentations were then compared with the assessors' manual segmentations and the automatic segmentations for further interobserver reliability. For a video of the manually corrected segmentation process, see Video 2.

Statistical Analysis

The Shapiro Wilks test was used to assess normal distribution. Differences in assessment times, intracranial, brain, and CSF volumes between healthy individuals and iNPH patients were tested with the independent samples *t* test. Non-normally distributed parameters were tested with the Mann Whitney U-test. Sex distribution among groups was tested with the χ^2 test. Differences between all 3 groups regarding age, EI, CA, Radscale score, and ventricular volumes were tested with one-way analysis of variance and Tukey post-hoc test. Association between parameters was investigated with Pearson's correlation analysis, assuming linear correlation. Intra- and interrater agreement were calculated with intraclass correlation coefficient (ICC) for continuous data using SPSS (IBM, Armonk, NY). Models used were 2-way mixed effects, absolute agreement, single rater/measurement, ICC (3,1) for intrarater reliability and 2-way mixed effects, absolute agreement, multiple raters/measurements (ICC, 3, k) for interrater reliability.³¹ A level of $P < 0.05$ was considered statistically significant. Statistical analyses were carried out using SPSS Statistics for Windows version 29.

RESULTS

All demographic and radiographic parameters, except for Radscale and CA, were normally distributed. Study demographics, including traditional radiologic measures, are displayed in **Table 1**. There was no difference in age or sex distribution among groups. EI was similar in shunted and non-shunted iNPH groups, while Radscale and CA were different between all groups ($P < 0.001$). Total intracranial CSF, BPF%, and ratio between ventricular volume and total intracranial CSF were all significantly different between healthy individuals and non-shunted iNPH patients ($P < 0.001$). Mean ventricular volumes were significantly smaller in shunted iNPH patients ($P < 0.05$) compared with non-shunted patients. All volumes generated automatically by the SyMRI software are shown in **Table 2**.

All segmentations of ventricular volume and time expenditure are shown in **Table 3**. Average time for the first manual segmentation round was 16:52 minutes for assessor 1 and 34:47 minutes for assessor 2. Average time for assessor 1's manual retest was 12:36 minutes, which is 25% less than the first round ($P < 0.001$). There was a further 58% time reduction when manually correcting automatic segmentations, averaging 5:17 minutes for assessor 1 ($P < 0.001$). There was an 80% time reduction for assessor 2, when correcting the automatic segmentations, with an average of 6:52 minutes ($P < 0.001$). The average time of assessors 1 and 2 correcting automatic segmentations was 6:05 minutes.

The difference between corrected mean total ventricular volume of all patients was 1.0 mL between assessors 1 and 2—98.1 and 97.1 mL, respectively. The mean automatic segmentation was 96.5 mL. Differences were non-significant with a general trend for automatic segmentations to be slightly smaller on average. However, intra- and interobserver reliability for all segmentations of ventricular volume was excellent with an ICC of 0.999 to 1.000, as shown in **Table 4**. Correlation between manually corrected and automatic ventricular volume was very good (Pearson = 0.998) shown in **Figure 2**. In both graphs there were 2 significant

Table 1. Demographic and Radiographic Data of Patients and Healthy Individuals

	Whole Group N = 45	Healthy Individuals N = 15	iNPH n = 15	Shunted iNPH N = 15
Age (years)	75 (62–85)	75 (65–81)	73 (62–85)	77 (63–82)
Sex (male/female, % female)	19/24 (58)	6/9 (60)	7/8 (53)	6/9 (60)
iNPH scale	n/a	n/a	46 (25–87)	60 (44–93)†
Radscale	6 (1–12)	2 (0–7)	9 (7–12)*	6 (4–10)*, †
Evans index	0.35 (0.26–0.43)	0.28 (0.23–0.32)	0.37 (0.3–0.43)*	0.36 (0.29–0.43)*
Callosal angle	95 (56–141)	124 (89–141)	75 (56–93)*	105 (73–126)*, †

Values are presented as median (range) or numbers and proportions. Level of significance $P < 0.01$.
 *Significant difference compared with healthy individuals.
 †Significant difference compared with iNPH group.

Table 2. Volumetric Data from the qMRI Software

qMRI Software Generated Volumes					
	Intracranial Volume (ICV)	Brain Parenchyma Volume (BPV)	Total Intracranial CSF	Ventricle Segmentation Mask/total Intracranial CSF	Brain Parenchyma Fraction (%)
Healthy individuals (n = 15)	1409 (136)	1087 (97)	323 (77)	0.13 (0.11)	77.2 (2.8)
iNPH (n = 15)	1471 (141)	1066 (108)	402 (68)*	0.35 (0.06)*	72.7 (3.3)*
Difference in iNPH group compared with healthy individuals	4.4%	-1.9%	24.5%	269%	-5.8%

Values are volumes in mL, mean (standard deviation).
 ICV, intracranial volume; BPV, brain parenchyma volume; BPF%, brain parenchymal fraction.
 *Significant difference compared with healthy individuals ($P < 0.001$).

outliers: both of them had cavum septum pellucidum et vergae, where the automatic algorithm identified the cavum as part of the ventricular system. Ventricular volume was miscalculated by 9.7 and 11.4 mL, respectively. Correlation between assessor 1 and assessor 2 corrected segmentations of ventricular volume was excellent (Figure 3). Pearson correlation and ICC was 1.000.

There was a positive correlation between EI and ventricular volume with a Pearson score of 0.875. A large variation can be observed though, as some patients with identical EI showed a difference in ventricular volumes with up to a factor 2 (Figure 4).

DISCUSSION

In this study we assessed the reliability of manual, automatic, and corrected automatic ventricular volumetry using 3D qMRI. Overall, we found excellent intra- and interobserver reliability, with an ICC of 0.999 to 1.000 across all segmentation methods. This is slightly

higher than in recent studies by Yamada et al. and Quon et al. comparing manual and automatic segmentations.^{7,32} Manual segmentations proved to be time-consuming, but with a significant improvement after the application of the automatic algorithm for ventricular volumetry.

Our study shows the shortcomings of EI in hydrocephalus follow-up demonstrated in the large variation depicted in Figure 4. This emphasizes the need for alternatives, as stated by Toma et al.⁶ While EI was similar between the non-shunted and shunted iNPH patient groups, ventricular volumes were clearly different. This distinction, especially since the non-shunted and shunted patient groups in our study were not identical, indicates the promising potential of ventricular segmentation using qMRI to evaluate shunt effectiveness in future research. Earlier studies have shown a strong correlation between ventricular volume and EI, but also significant variation among patients.³³ We found significant differences in both CA and overall Radscale score

Table 3. Volumetric Data and Time Expenditure

	Assessor 1			Assessor 2		Automatic Ventricular Segmentation = 45
	Manual Test n = 45	Manual Retest n = 45	Corrected n = 45	Manual Test n = 15	Corrected n = 45	
Healthy individuals	42.6 (18.4)	42.5 (18.4)	41.8 (18.3)	44.4 (22.8)	41.0 (18.0)	39.8 (18.2)
iNPH	140.9 (33.7) *	140.8 (33.8) *	139.9 (33.6) *	157.7 (28.2) *	138.8 (33.4) *	138.3 (31.8) *
Shunted iNPH	113.4 (34.9) *,†	113.2 (35.2) *,†	112.6 (34.9) *,†	90.0 (25.3) *,†	111.6 (35.0) *,†	111.4 (34.0) *,†
Average time for segmentation (min:sec)	16:52	12:36	5:17	34:47	6:52	0:01
Time cut (%)	n/a	25%	58%	n/a	80%	

Values are ventricular volumes in mL, mean (standard deviation).
 n/a, not applicable.
 *Significant difference compared with healthy subjects ($P < 0.001$).
 †Significant difference compared with iNPH group ($P < 0.05$).

Table 4. Intraclass Correlation Coefficient (ICC) for Continuous Data of Ventricular Volume Segmentation

Intra Class Correlation - ICC					
	Assessor 1 Manual Test	Assessor 1 Manual retest	Assessor 1 Corrected	Assessor 2 Manual Test	Assessor 2 Corrected
Assessor 1 manual retest	1.000 (1.000–1.000)				
Assessor 1 corrected	1.000 (0.999–1.000)	1.000 (0.999–1.000)			
Assessor 2 manual test	1.000 (0.994–1.000)	1.000 (0.988–1.000)	1.000 (0.999–1.000)		
Assessor 2 corrected	1.000 (0.980–1.000)	1.000 (0.975–1.000)	1.000 (0.998–1.000)	1.000 (1.000–1.000)	
Automatic algorithm	0.999 (0.992–0.999)	0.999 (0.993–0.999)	0.999 (0.997–1.000)	0.999 (0.997–1.000)	0.999 (0.998–1.000)

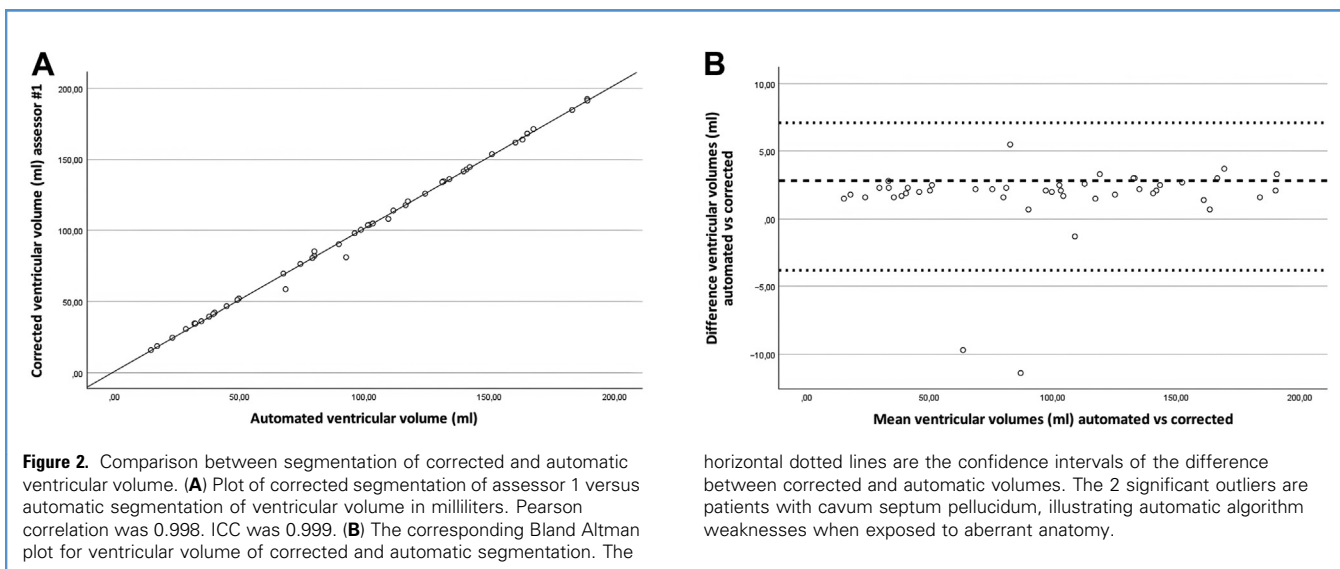
Values presented are ICC average measures and their 95% confident intervals (lower bound–upper bound). Models used are 2-way mixed effects, absolute agreement, single rater/measurement, ICC (3,1) for intra-rater reliability (cursivated) and 2-way mixed effects, absolute agreement, multiple raters/measurements (ICC, 3, k) for inter-rater reliability.³¹

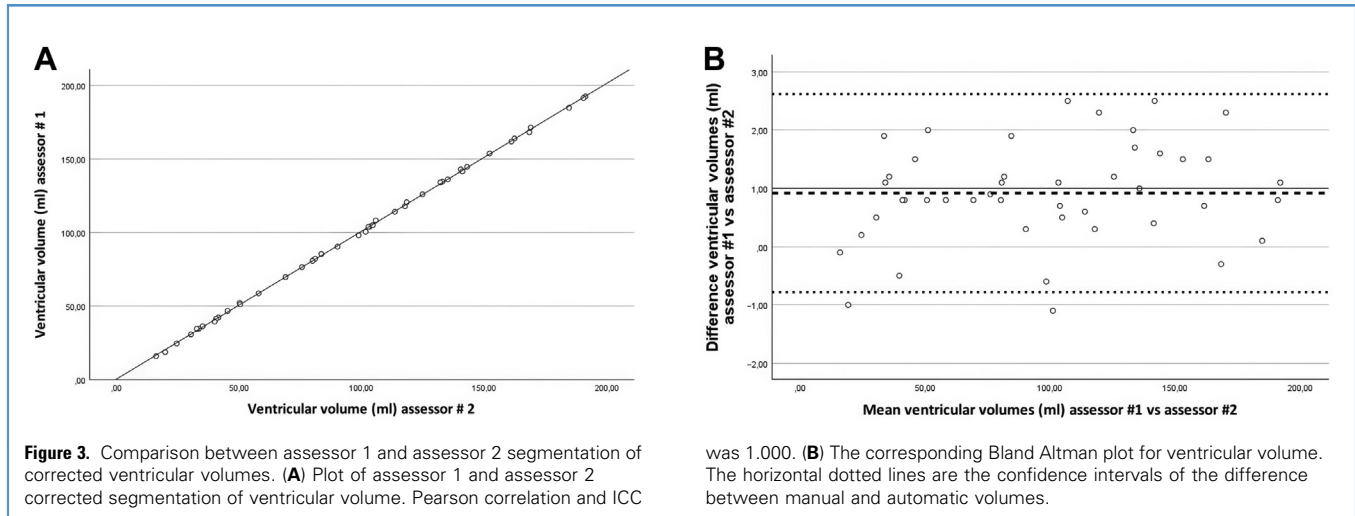
between shunted and non-shunted iNPH-patients in this study, as seen in **Table 1**. A previous study has also shown an increase of CA along with a decrease in ventricular volume after shunt surgery.³⁴

Ventricular volume has recently been shown to be more strongly associated with clinical improvement than EI after shunting in iNPH.⁹ Crooks et al. found a strong association between ventricular volume, gait, and cognition.³⁵ Specifically, the ratios between frontal horn volume to total ICV and ventricular volume to ICV were significantly correlated with function, independent of EI in the same patients. In this study, we introduce a ratio between ventricular volume and total intracranial CSF, which clearly separates healthy individuals from those with ventriculomegaly (**Table 2**). The ratio was increased by 269% in the iNPH group compared with healthy individuals. We believe this ratio potentially could be used to identify patients at risk of

developing hydrocephalus and monitor the progression of hydrocephalus and other diseases with ventriculomegaly.

Numerous CT- and MRI-based software tools allow manual or semi-automatic ventricular segmentation.^{10,36} Not only does time-expenditure limit the usefulness of manual segmentation, but also thresholding differences in traditional MRI acquisition can introduce sources of error when segmenting CSF. Yepes-Calderon and McComb recently questioned the efficacy, precision, and reliability of using conventional T1- or T2-weighted images as the “ground truth” for segmentation due to these issues.³⁷ Currently, there is no consensus on a gold standard or reference method to test other software tools against. Cross-sectional comparisons of 3D MRI volumetry segmentation tools in several studies have yielded diverging results.^{15,38,39} Also, impaired reproducibility across scanners is an issue hampering clinical implementation and hindering multicenter studies.^{15,40} Quantitative MRI circumvents



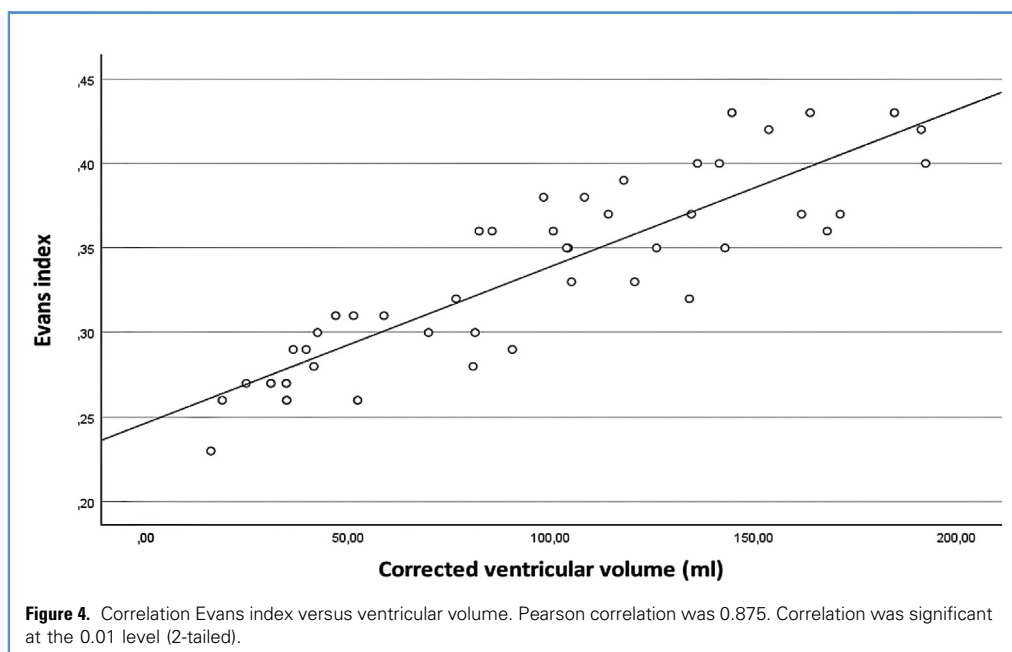


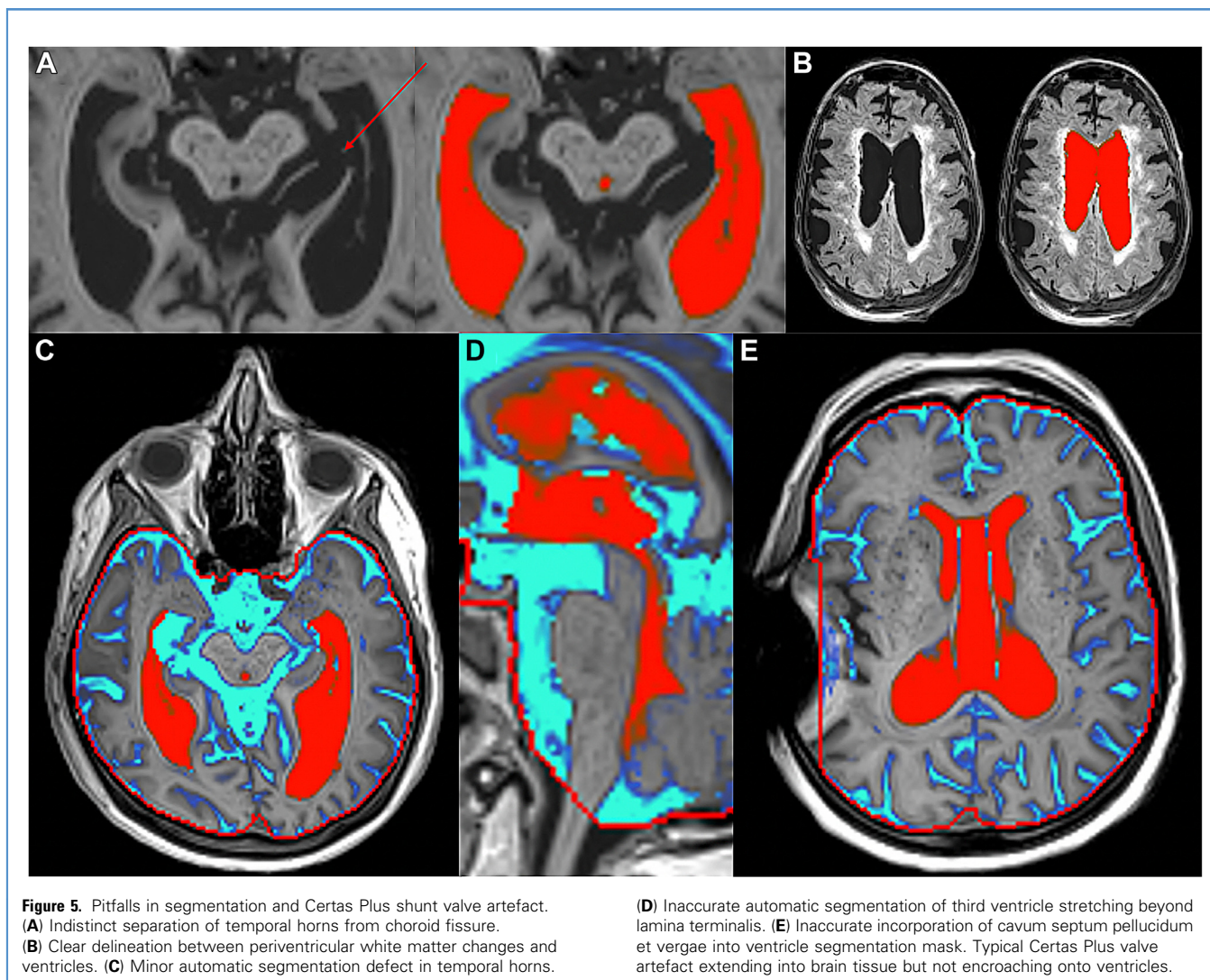
these issues by directly calculating CSF volumes from quantitative maps, avoiding threshold-based errors and ensuring consistency across different machines and settings. This may reduce potential differences that occur in conventional images acquired on different vendors and using different scanner settings.

To overcome time-consuming manual segmentation, several automatic algorithms have been developed.^{8,32,41} Automatic algorithms often face limitations in segmenting ventricles, given their complex anatomical relationships to the basal cisterns and frequently aberrant anatomy introducing systematic errors.⁴² Therefore, many tools settle for lateral ventricle

segmentation.^{34,35} However, segmentation of the whole ventricular system is necessary as many complex patients, especially with obstructive hydrocephalus, will have variable enlargement and reduction of separate ventricles.

There are pitfalls and challenges in both manual and automatic segmentation. Manual segmentation of the ventricular system is user-dependent and requires in-depth knowledge of ventricular anatomy, especially in defining the third ventricle and its anterior, superior, and posterior boundaries. Also, delineating the temporal horns from the choroid fissure can be challenging. In our study, the automatic algorithm tended to underestimate ventricular





volumes, occasionally missing minor parts of specific anatomical regions, such as the temporal horns. Automatic segmentations could also extend beyond the bottom of the third ventricle (Figure 5). From a statistical perspective, this did not significantly alter the accuracy of automatic segmentations in relation to manual, as the differences were miniscule, most often less than 0.1 mL. However, in a potential subgroup analysis of each ventricle, this limitation could have a significant effect. In our cohort, 2 patients had cavum septum pellucidum et vergae, which the algorithm recognized as a part of the ventricular system (Figure 5). Additionally, CSF-filled porencephalic cavities that communicated with the ventricular system were also misinterpreted as part of ventricles. This underscores that major deviations from normal ventricular anatomy can influence the outcome of automatic segmentation. At this point, we still see the need for a human hydrocephalus clinician or radiologist to review the MRI exams for major errors. However, continued software

development that accounts for and recognizes the most common developmental and pathologic anomalies in ventricles should help overcome this problem. We would like to note that cavum septum pellucidum et vergae has since been addressed by the developers, and, in later software versions, the algorithm can recognize this anomaly (unpublished results).

Even though the software was easy to learn and intuitive to use, the image resolution of 3D-QALAS was satisfactory but inferior to conventional T₁ and T₂ images. This difference became especially apparent when assessing very thin membranes at the borders of ventricles. For instance, lamina terminalis could not be visualized in many scans, making the delineation of the anterior boundary of the third ventricle cumbersome. If generalized to other patient groups, this issue could impose problems when assessing patients with membranous aqueductal stenosis or multiple thin-walled arachnoid cysts. In this regard, conventional volumetry from 3D T₁ sequences is superior. For 3D-QALAS to achieve equivalent

accuracy, improvement in image resolution and slice thickness would be necessary. Indeed, SyMRI has been shown to be qualitatively inferior to conventional MRI.⁴³ However, this does not significantly impact clinical outcomes.⁴⁴ While we recognize this limitation, we also emphasize that most previous studies have used the 2D equivalent of qMRI rather than 3D-QALAS. Furthermore, the scope of the present study was not to assess brain lesions but to harness the ability of this technique to quantify CSF, enabling its use for ventricular segmentation. In operated patients, the Certas Plus shunt artifact extended to the brain parenchyma (Figure 5), but it never interfered with the lateral ventricles, consistent with the findings of Camerucci et al.²⁵ Periventricular white matter changes can also be challenging to delineate from ventricular CSF in classical MRI segmentation. However, in qMRI, the algorithm can easily separate them, as their tissue properties differ from CSF (Figure 5).

There are limitations to this study. Our subgroups may appear to be small, without prospective follow-up of patients after shunting. However, this is an initial effort to assess the accuracy of ventricular volumetry with qMRI, before the method is applied in a broader cohort. The volumetric measurements did not include a phantom with known volume, as this already had been performed in the evaluation of 3D-QALAS by Fujita et al., showing strong linearity with the reference values.²¹ Our measurements were not compared with another traditional segmentation software as this practice is strongly discouraged due to methodologic problems as described by McComb et al.³⁷ Images were only acquired once so we could not calculate scan–rescan reproducibility. Scanner variability in 3D-QALAS data acquisition would have to be addressed in a multi-center study setting. Algorithm development was conducted using a series of segmentations of normally configured and enlarged ventricles in iNPH patients. However, it has not been applied to hydrocephalus of other etiologies and, thus, cannot be generalized at this point. Continued software development and validation studies, similar to this one, in cohorts with pediatric and obstructive hydrocephalus patients could demonstrate its utility in a larger clinical setting. Especially children could benefit from the short scan time offered by 3D-QALAS and avoid the need for prolonged sedation. With repeated scans using the same software algorithm on the same patient, the clinical implications of the observed differences between manual and automatic segmentation are expected to be minimal. We

believe this automated software algorithm shows promise for longitudinal monitoring of hydrocephalus patients, with repeated scans over time to evaluate the effects of shunting and detect shunt failure.⁴⁵ Patients with very large ventricles and thin cortical brain mantle could benefit from 3D-QALAS ventricular volumetry, as linear 2D measurements often remain unchanged, even after successful shunting, based on our experience. Moreover, monitoring the expansion of arachnoid cysts presents another potential clinical application.

Future studies should focus on evaluating longitudinal volumetric changes in iNPH and how ventricular volumes correlate with the clinical outcome. Moreover, the efficacy of the ratio between ventricular volume and total intracranial CSF in monitoring hydrocephalus and brain atrophy should be explored in prospective cohorts. Future developments should also focus on automatic volumetric analysis of CSF in focally enlarged sulci and among tight high-convexity sulci.

The implementation of the automatic algorithm significantly enhanced the segmentation process, offering a helpful template for examiner correction. Few automatic algorithms can identify and segment the whole ventricular system in a reliable way, and, to our knowledge, no existing quantitative MRI-based software fulfills this function.

CONCLUSIONS

In conclusion, we assert that the used segmentation software paired with the 3D-QALAS sequence is a reliable and efficient method for obtaining relevant volumetric measures of intracranial CSF spaces, showcasing promise for both clinical and research purposes.

CRediT AUTHORSHIP CONTRIBUTION STATEMENT

Rafael T. Holmgren: Conceptualization, Data curation, Formal analysis, Funding acquisition, Methodology, Project administration, Validation, Visualization, Writing – original draft. **Anders Tisell:** Data curation, Methodology, Project administration, Writing – review & editing. **Marcel J.B. Warntjes:** Formal analysis, Methodology, Software, Validation, Writing – review & editing. **Charalampos Georgiopoulos:** Conceptualization, Formal analysis, Investigation, Methodology, Supervision, Validation, Writing – review & editing.

REFERENCES

- Meier U, Mutze S. Correlation between decreased ventricular size and positive clinical outcome following shunt placement in patients with normal-pressure hydrocephalus. *J Neurosurg.* 2004; 100:1036-1040.
- Meier U, Paris S, Gräwe A, Stockheim D, Hajdukova A, Mutze S. Is there a correlation between operative results and change in ventricular volume after shunt placement? A study of 60 cases of idiopathic normal-pressure hydrocephalus. *Neuroradiology.* 2003;45:377-380.
- Synek V, Reuben JR, Du Boulay GH. Comparing Evans' index and computerized axial tomography in assessing relationship of ventricular size to brain size. *Neurology.* 1976;26:231-233.
- Evans WJ. An encephalographic ratio for estimating ventricular enlargement and cerebral atrophy. *Arch Neurol Psychiatry.* 1942;47:931-937, 1942.
- Marmarou A, Bergsneider M, Relkin N, Klinge P, Black PM. Development of guidelines for idiopathic normal-pressure hydrocephalus: introduction. *Neurosurgery.* 2005;57(3 Suppl):S1-S3 [discussion: ii-v].
- Toma AK, Holl E, Kitchen ND, Watkins LD. Evans' index revisited: the need for an alternative in normal pressure hydrocephalus. *Neurosurgery.* 2011;68:939-944.
- Yamada S, Otani T, Ii S, et al. Aging-related volume changes in the brain and cerebrospinal fluid using artificial intelligence-automated segmentation. *Eur Radiol.* 2023;33:7099-7112.
- Kellogg RT, Park MS, Snyder MH, et al. Establishment of age- and sex-specific reference cerebral ventricle volumes. *World neurosurgery.* 2023; 175:e976-e983.
- Neikter J, Agerskov S, Hellström P, et al. Ventricular volume is more strongly associated with clinical improvement than the Evans index after shunting in idiopathic normal pressure hydrocephalus. *AJNR Am J Neuroradiol.* 2020;41: 1187-1192.

10. Fischl B. FreeSurfer. *Neuroimage*. 2012;62:774-781.
11. Gaser C, Dahnke R, Thompson PM, Kurth F, Luders E. The Alzheimer's Disease Neuroimaging I. CAT: a computational anatomy toolbox for the analysis of structural MRI data. *GigaScience*. 2024; 13:giaeo49.
12. Henschel L, Conjeti S, Estrada S, Diers K, Fischl B, Reuter M. FastSurfer - a fast and accurate deep learning based neuroimaging pipeline. *Neuroimage*. 2020;219:117012.
13. Fedorov A, Beichel R, Kalpathy-Cramer J, et al. 3D slicer as an image computing platform for the quantitative imaging network. *Magn Reson Imaging*. 2012;30:1323-1341.
14. Brewer JB. Fully-automated volumetric MRI with normative ranges: translation to clinical practice. *Behav Neurol*. 2009;21:21-28.
15. van Nderpelt DR, Amiri H, Brouwer I, et al. Reliability of brain atrophy measurements in multiple sclerosis using MRI: an assessment of six freely available software packages for cross-sectional analyses. *Neuroradiology*. 2023;65: 1459-1472.
16. Fujita S, Hagiwara A, Takei N, et al. Accelerated isotropic multiparametric imaging by high spatial resolution 3D-QALAS with compressed sensing: a phantom, volunteer, and patient study. *Invest Radiol*. 2021;56:292-300.
17. Seiler A, Nöth U, Hok P, et al. Multiparametric quantitative MRI in neurological diseases. *Front Neurol*. 2021;12:640239.
18. Virhammar J, Warntjes M, Laurell K, Larsson EM. Quantitative MRI for rapid and user-independent monitoring of intracranial CSF volume in hydrocephalus. *AJNR Am J Neuroradiol*. 2016;37:797-801.
19. Ambarki K, Lindqvist T, Wahlin A, et al. Evaluation of automatic measurement of the intracranial volume based on quantitative MR imaging. *AJNR Am J Neuroradiol*. 2012;33:1951-1956.
20. Fujita S, Hagiwara A, Hori M, et al. Three-dimensional high-resolution simultaneous quantitative mapping of the whole brain with 3D-QALAS: an accuracy and repeatability study. *Magn Reson Imaging*. 2019;63:235-243.
21. Fujita S, Hagiwara A, Hori M, et al. 3D quantitative synthetic MRI-derived cortical thickness and subcortical brain volumes: scan-rescan repeatability and comparison with conventional T1-weighted images. *J Magn Reson Imaging*. 2019;50: 1834-1842.
22. Warntjes JBM, Lundberg P, Tisell A. Brain parcellation repeatability and reproducibility using conventional and quantitative 3D MR imaging. *Am J Neuroradiol*. 2023;44:910-915.
23. Eklund A, Koskinen LO, Williams MA, Luciano MG, Dombrowski SM, Malm J. Hydrodynamics of the Certas™ programmable valve for the treatment of hydrocephalus. *Fluids Barriers CNS*. 2012;9:12.
24. Shellock FG, Bedwinek A, Oliver-Allen M, Wilson SF. Assessment of MRI issues for a 3-T "immune" programmable CSF shunt valve. *AJR Am J Roentgenol*. 2011;197:202-207.
25. Camerucci E, Elder BD, Shu Y, et al. Field strength difference in extent of artifacts induced by CERTAS Plus valves in patients with idiopathic normal pressure hydrocephalus. *NeuroRadiol J*. 2023;36: 665-673.
26. Hellstrom P, Klinge P, Tans J, Wikkelso C. A new scale for assessment of severity and outcome in iNPH. *Acta Neurol Scand*. 2012;126:229-237.
27. Tisell A, Warntjes M, Lundberg P, Testud F. 3D quantitative MRI of the brain: effect of B1 inhomogeneity in 3D-QALAS. *ISMRM*; May 15-20; 2021. Available at: <https://archive.ismrm.org/2021/1291.html>. Accessed January 28, 2025.
28. Kvernby S, Warntjes MJ, Haraldsson H, Carlhäll CJ, Engvall J, Ebbens T. Simultaneous three-dimensional myocardial T1 and T2 mapping in one breath hold with 3D-QALAS. *J Cardiovasc Magn Reson*. 2014;16:102.
29. West J, Warntjes JB, Lundberg P. Novel whole brain segmentation and volume estimation using quantitative MRI. *Eur Radiol*. 2012;22:998-1007.
30. Kockum K, Lilja-Lund O, Larsson EM, et al. The idiopathic normal-pressure hydrocephalus rad-scale: a radiological scale for structured evaluation. *Eur J Neurol*. 2018;25:569-576.
31. Koo TK, Li MY. A guideline of selecting and reporting intraclass correlation coefficients for reliability research. *J Chiropr Med*. 2016;15:155-163.
32. Quon JL, Han M, Kim LH, et al. Artificial intelligence for automatic cerebral ventricle segmentation and volume calculation: a clinical tool for the evaluation of pediatric hydrocephalus. *J Neurosurg Pediatr*. 2020;27:131-138.
33. Ambarki K, Israelsson H, Wahlin A, Birgander R, Eklund A, Malm J. Brain ventricular size in healthy elderly: comparison between Evans index and volume measurement. *Neurosurgery*. Jul 2010;67: 94-99 [discussion: 99].
34. Virhammar J, Laurell K, Cesarini KG, Larsson EM. Increase in callosal angle and decrease in ventricular volume after shunt surgery in patients with idiopathic normal pressure hydrocephalus. *J Neurosurg*. 2018;130:1-6.
35. Crook JE, Gunter JL, Ball CT, et al. Linear vs volume measures of ventricle size: relation to present and future gait and cognition. *Neurology*. 2020;94: e549-e556.
36. Yushkevich PA, Yang G, Gerig G. ITK-SNAP: an interactive tool for semi-automatic segmentation of multi-modality biomedical images. *Annu Int Conf IEEE Eng Med Biol Soc*. 2016;2016:3342-3345.
37. Yepes-Calderon F, McComb JG. Eliminating the need for manual segmentation to determine size and volume from MRI. A proof of concept on segmenting the lateral ventricles. *PLoS One*. 2023; 18:e0285414.
38. Heo YJ, Baek HJ, Skare S, et al. Automated brain volumetry in patients with memory impairment: comparison of conventional and ultrafast 3D T1-weighted MRI sequences using two software packages. *AJR American journal of roentgenology*. 2022;218:1062-1073.
39. Koussis P, Toulas P, Glotsos D, Lamprou E, Kehagias D, Lavdas E. Reliability of automated brain volumetric analysis: a test by comparing NeuroQuant and volBrain software. *Brain Behav*. 2023;13:e3320.
40. Liu S, Hou B, Zhang Y, et al. Inter-scanner reproducibility of brain volumetry: influence of automated brain segmentation software. *BMC Neurosci*. 2020;21:35.
41. Wang Y, Feng A, Xue Y, et al. Automated ventricle PARCELLATION and EVAN'S ratio COMPUTATION IN PRE- and post-surgical ventriculomegaly. *Proc IEEE Int Symp Biomed Imaging*. 2023;2023:1-5.
42. Ziegelitz D, Hellström P, Björkman-Burtscher IM, et al. Evaluation of a fully automated method for ventricular volume segmentation before and after shunt surgery in idiopathic normal pressure hydrocephalus. *World neurosurgery*. 2024;181: e303-e311.
43. Di Giuliano F, Minosse S, Picchi E, et al. Comparison between synthetic and conventional magnetic resonance imaging in patients with multiple sclerosis and controls. *Magma*. 2020;33: 549-557.
44. Krauss W, Gunnarsson M, Nilsson M, Thunberg P. Conventional and synthetic MRI in multiple sclerosis: a comparative study. *Eur Radiol*. 2018;28:1692-1700.
45. Lidén S, Farahmand D, Laurell K. Volumetric effect of shunt adjustments in normal pressure hydrocephalus: a randomized, double-blind trial. *J Neurosurg*. 2023;140:1-8.

Preliminary results from this article were presented at Hydrocephalus 2023, August 25–28, 2023, annual meeting of the International Society of Hydrocephalus and Cerebrospinal Fluid Disorders.

Conflict of interest statement: The study was supported by Linköping University Hospital Research Fund. J.B.M. Warntjes reports a relationship with SyntheticMR AB that includes: board membership, consulting or advisory, and equity or stocks. JBM Warntjes has patent 'Methods and Systems for Improved Magnetic Resonance Acquisition', US2015177350 (A1)/US10073156 (B2) issued to SyntheticMR AB. If there are other authors, they declare that they have no known competing financial interests or personal relationships that could have appeared to influence the work reported in this paper.

Received 22 December 2024; accepted 4 January 2025

Citation: World Neurosurg. (2025) 195:123661. <https://doi.org/10.1016/j.wneu.2025.123661>

Journal homepage: www.journals.elsevier.com/world-neurosurgery

Available online: www.sciencedirect.com

1878-8750/© 2025 The Author(s). Published by Elsevier Inc. This is an open access article under the CC BY license (<http://creativecommons.org/licenses/by/4.0/>).